

RESEARCH

Open Access



# Dissecting the genetic basis of UV-B responsive metabolites in rice

Feng Zhang<sup>1,2</sup>, Chenkun Yang<sup>3</sup>, Hao Guo<sup>3</sup>, Yufei Li<sup>3</sup>, Shuangqian Shen<sup>3</sup>, Qianqian Zhou<sup>2</sup>, Chun Li<sup>3</sup>, Chao Wang<sup>3</sup>, Ting Zhai<sup>1</sup>, Lianghuan Qu<sup>2</sup>, Cheng Zhang<sup>1</sup>, Xianqing Liu<sup>3</sup>, Jie Luo<sup>3,4</sup>, Wei Chen<sup>2,5</sup>, Shouchuang Wang<sup>3,4</sup>, Jun Yang<sup>3\*</sup>, Cui Yu<sup>1\*</sup> and Yanyan Liu<sup>2,5\*</sup>

\*Correspondence:  
yang9yj@hainanu.edu.cn;  
yucui@hbaas.com;  
liuyanyan@mail.hzau.edu.cn

<sup>1</sup> Industrial Crops Institute, Hubei Academy of Agricultural Sciences, Wuhan, Hubei 430064, China

<sup>2</sup> National Key Laboratory of Crop Genetic Improvement, Huazhong Agricultural University, Wuhan, Hubei 430070, China

<sup>3</sup> School of Breeding and Multiplication (Sanya Institute of Breeding and Multiplication), Hainan University, Sanya, Hainan 572025, China

<sup>4</sup> Yazhouwan National Laboratory, Sanya, Hainan 572025, China

<sup>5</sup> Hubei Hongshan Laboratory, Wuhan, Hubei 430070, China

## Abstract

**Background:** UV-B, an important environmental factor, has been shown to affect the yield and quality of rice (*Oryza sativa*) worldwide. However, the molecular mechanisms underlying the response to UV-B stress remain elusive in rice.

**Results:** We perform comprehensive metabolic profiling of leaves from 160 diverse rice accessions under UV-B and normal light conditions using a widely targeted metabolomics approach. Our results reveal substantial differences in metabolite accumulation between the two major rice subspecies *indica* and *japonica*, especially after UV-B treatment, implying the possible role and mechanism of metabolome changes in subspecies differentiation and the stress response. We next conduct a transcriptome analysis from four representative rice varieties under UV-B stress, revealing genes from amino acid and flavonoid pathways involved in the UV-B response. We further perform a metabolite-based genome-wide association study (mGWAS), which reveals 3307 distinct loci under UV-B stress. Identification and functional validation of candidate genes show that *OsMYB44* regulates tryptamine accumulation to mediate UV-B tolerance, while *OsUVR8* interacts with *OsMYB110* to promote flavonoid accumulation and UV-B tolerance in a coordinated manner. Additionally, haplotype analysis suggests that natural variation of *OsUVR8*<sup>groupA</sup> contributes to UV-B resistance in rice.

**Conclusions:** Our study reveals the complex biochemical and genetic foundations that govern the metabolite dynamics underlying the response, tolerance, and adaptive strategies of rice to UV-B stress. These findings provide new insights into the biochemical and genetic basis of the metabolome underlying the crop response, tolerance, and adaptation to UV-B stress.

**Keywords:** UV-B stress, Metabolome, Transcriptome, mGWAS, Genetic basis, Natural variation, Rice



© The Author(s) 2024. **Open Access** This article is licensed under a Creative Commons Attribution-NonCommercial-NoDerivatives 4.0 International License, which permits any non-commercial use, sharing, distribution and reproduction in any medium or format, as long as you give appropriate credit to the original author(s) and the source, provide a link to the Creative Commons licence, and indicate if you modified the licensed material. You do not have permission under this licence to share adapted material derived from this article or parts of it. The images or other third party material in this article are included in the article's Creative Commons licence, unless indicated otherwise in a credit line to the material. If material is not included in the article's Creative Commons licence and your intended use is not permitted by statutory regulation or exceeds the permitted use, you will need to obtain permission directly from the copyright holder. To view a copy of this licence, visit <http://creativecommons.org/licenses/by-nc-nd/4.0/>.

## Background

Ultraviolet-B (UV-B; 280–315 nm) is a crucial environmental factor that poses a threat to plant growth, development, and crop yield due to the depletion of the stratospheric ozone layer, with strong UV-B radiation inducing particularly harmful effects [1, 2]. Furthermore, the levels of UV-B on the Earth's surface have increased by 6–14% since the 1980s due to declining ozone levels in the atmosphere [3, 4]. Although UV-B accounts for only a small portion of the total solar radiation, its impact on plants can be significant, causing changes at the molecular, cellular, morphological, and physiological levels [5, 6]. Studies have demonstrated that elevated UV-B radiation shows a strong negative linear correlation with rice biomass production and yields [7, 8]. As UV-B levels continue to rise, decreased rice yields are inescapable, which would ultimately increase the demand for world rice production. Thus, understanding the regulation mechanism of the response and tolerance to UV-B in rice is crucial.

The perception and response to UV-B stress are complex processes regulated by multiple loci and are influenced by various environmental factors such as latitude, season, solar angle, and atmosphere thickness in plants [9, 10]. It has been reported that the responses to lower doses of UV-B are at least partially mediated by the UV-B-specific UV RESISTANCE LOCUS 8 (UVR8) photoreceptor to regulate gene expression, whereas the responses to higher doses of UV-B involve various regulatory mechanisms, including the UVR8-independent pathway, cellular damage, and reactive oxygen species-mediated oxidative stress [11–14]. To respond to the complexity of UV-B stress perception, plants have evolved diverse defensive strategies, including increased levels of UV-B-absorbing sunscreens in the vacuoles of epidermal cells, antioxidant accumulation, and photosynthetic apparatus protection [15, 16]. Among these protective mechanisms, the accumulation of UV-B-absorbing sunscreens in the vacuoles of epidermal cells represents a particularly important adaptation of higher plants [17, 18]; these sunscreens mainly comprise phenolic compounds such as flavonoids, anthocyanins, and hydroxycinnamic acids [17, 19]. UV-B also has a marked effect on the levels of amino acids, lipids, and terpenoids in many plants [20–22]. However, the genetic basis of the regulation of these metabolites underlying the plant response to UV-B stress is still not well understood.

In nature, plants produce thousands of unique metabolites playing essential roles in growth, development, and tolerance to biotic and abiotic stresses [23–25]. The changes in the levels of metabolites under stress exposure result from interactions between genotypes and the surrounding environment, largely reflecting the response, tolerance, and adaptation to stresses in plants. With the rapid development of next-generation sequencing technologies [26, 27], metabolite-based genome-wide association studies (mGWASs) have been widely used to reveal the genetic basis of metabolic diversity and variation in plants under various types of stress [28–30]. Differentially evolved glucosyltransferases such as *OsUGT706D1* (flavone 7-*O*-glucosyltransferase) and *OsUGT707A2* (flavone 5-*O*-glucosyl-transferase) were identified to determine the natural variation of flavone accumulation and UV tolerance in 529 rice accessions [31]. Global insights into the metabolic landscape and metabolite–gene associations have been revealed by combining large-scale untargeted mGWAS with time-course-derived networks under different abiotic environments for identifying metabolite–gene associations in *Arabidopsis* [32]. Co-selection of both constitutive and induced phenylpropanoids for the

UV-B response and protection has been demonstrated in diverse Qingke and other barley accessions [33]. Although rice is a major cereal crop responsible for feeding over half the world's population [34], the genetic basis of the metabolic diversity and adaptation to stress, especially UV-B stress, in rice remains unclear.

In this study, we conducted a comprehensive analysis of the metabolic and transcriptomic profiles of rice in response to UV-B stress. Our results demonstrated differences in metabolite accumulation between rice subspecies (*indica* and *japonica*) along with genes from amino acid and flavonoid pathways involved in the UV-B response. mGWAS analyses further revealed distinct loci that are specifically induced under UV-B stress. By identifying and functionally validating candidate genes, we discovered novel genes that play a role in the accumulation of metabolites to mediate UV-B tolerance. Moreover, haplotype analysis was used to reveal the specific genetic variations with a major contribution to conferring rice with improved UV-B tolerance. These results advance our understanding of the biochemical and genetic factors of metabolomes that underlie crop response, tolerance, and adaptation to UV-B stress.

## Results

### UV-B-responsive metabolic profiling in rice

To investigate the metabolic regulatory network in response to UV-B stress in rice seedlings, we collected leaf samples from 160 rice varieties grown under normal and high UV-B conditions, respectively (Additional file 2: Table S1), and analyzed them using an ultrahigh-performance liquid chromatography-tandem mass spectroscopy (UPLC-MS/MS)-based widely targeted metabolic profiling method as described previously [35, 36]. A total of 810 metabolic features were determined; among them, 143 were confirmed by comparison with standards and 326 were putatively annotated, including alkaloids, amino acids, fatty acids, flavonoids, hormones, nucleic acids, others, phenolamines, polyphenols, terpenes, and vitamins (Additional file 1: Fig. S1; Additional file 2: Table S2). Principal component analysis (PCA) of these metabolites showed a clear separation between the normal and UV-B treatment conditions along the first component, while the second component separated the *indica* and *japonica* subspecies, consistent with a previous report [28]. Interestingly, this subspecies separation was more pronounced under UV-B conditions, indicating a possible role and mechanism of metabolite regulation in subspecies differentiation and the stress response (Fig. 1a). Furthermore, differentially accumulated metabolite analysis between treated and control samples indicated that most (436/810) of the metabolites were significantly influenced by UV-B stress, namely 47.5% (385/810) metabolites showed upregulated patterns and 6.3% (51/810) displayed downregulated patterns ( $|\text{Fold Change}| \geq 5$ ,  $P < 0.05$ ) under the UV-B stress compared with normal conditions (Fig. 1b). Notably, these annotated and upregulated metabolites mainly belonged to amino acids, fatty acids, and flavonoids (Fig. 1c; Additional file 1: Fig. S2), indicating these metabolites might confer and control rice UV-B response and tolerance. Additionally, the cluster dendrogram based on differential accumulation of the metabolites showed two distinct groups under the UV-B conditions, in line with the PCA results (Fig. 1d). Collectively, these results suggest that the identified UV-B-responsive metabolites could efficiently reflect and even play substantial roles in the response and tolerance to UV-B in rice.

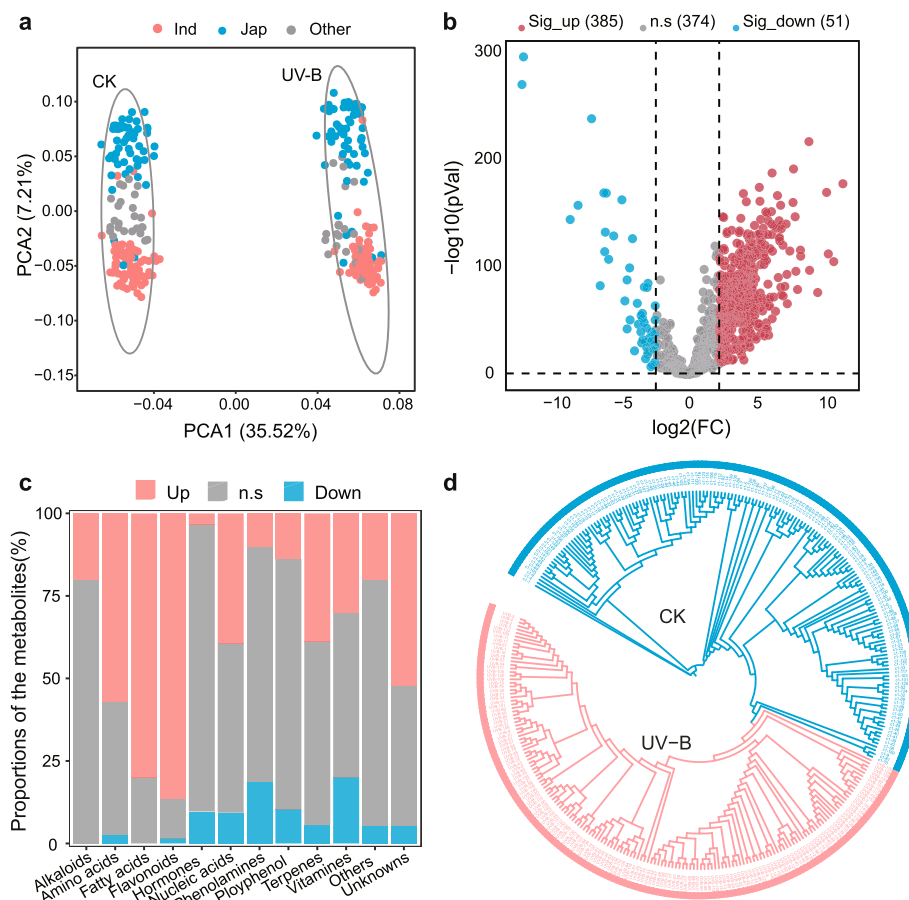


**Fig. 1** Metabolic differential accumulation of rice seedling leaves under normal and UV-B conditions. **a** Principal component analysis (PCA) of metabolites of rice seedling leaves under normal and UV-B conditions. **b** Volcano plot displaying upregulated and downregulated metabolites under UV-B conditions compared to those under the normal conditions; the red dot represents a metabolite with a  $|\text{Fold Change}| \geq 5$  and the blue dot represents a metabolite with a  $|\text{Fold Change}| \leq 0.2$ ,  $P \leq 0.05$ . **c** Percentage of differential metabolites identified under UV-B conditions compared to those under the normal conditions. **d** Neighbor-joining tree of 160 rice varieties based on 810 metabolites under normal and UV-B conditions

### UV-B-responsive transcriptomic profiling in rice

To better understand the mechanism underlying the UV-B-responsive metabolites in rice, we selected some rice varieties for UV-B tolerance analysis and found that different rice varieties showed distinct difference to UV-B tolerance (Additional file 1: Fig. S3). Further four rice varieties (two conventional varieties, ZH11 and ZS97, medium susceptible and medium resistant to UV-B stress respectively; a UV-B resistant variety, Lemon; and a UV-B susceptible variety, Dular) were used for transcriptome analysis under normal and UV-B conditions. PCA showed greater differences in gene expression levels between the normal and UV-B treatment conditions than among the four rice varieties, with the first component explaining 22.5% of the total variance (Fig. 2a). Comparative analysis of differentially expressed genes (DEGs) in these rice varieties under UV-B treatment revealed 9029 (3995 up-regulated and 5034 down-regulated), 7596 (3047 up-regulated and 4549 down-regulated), 7870 (3831 up-regulated and 4039 down-regulated), and 9296 (5251 up-regulated and 4045 down-regulated) DEGs in ZH11

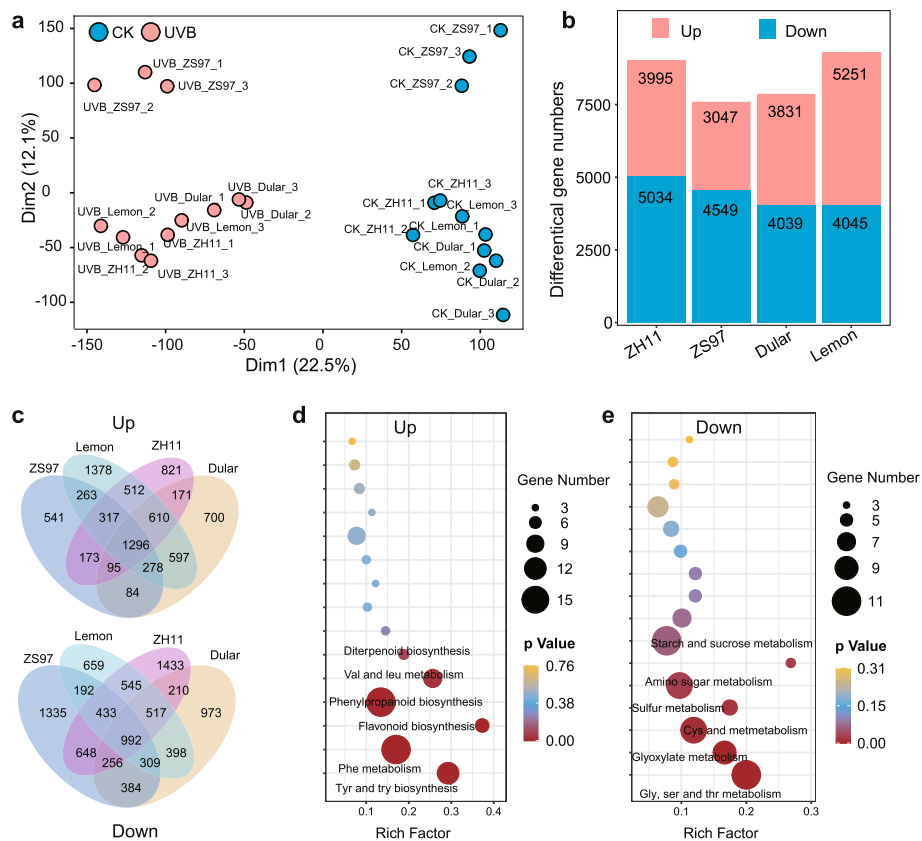


**Fig. 2** Global transcriptome responses in seedling leaves of four rice varieties under normal and UV-B conditions. **a** PCA of transcriptome reprogramming in seedling leaves of four rice varieties namely ZH11, ZS97, Lemon, and Dular under normal and UV-B conditions. **b** Number of differentially expressed genes (DEGs) in seedling leaves of four rice varieties under UV-B conditions; red, up-regulated genes and blue, down-regulated genes. **c** Venn diagrams showing overlap of DEGs in seedling leaves of four rice varieties under UV-B conditions. **d** KEGG pathway enrichment analysis for DEGs in seedling leaves of four rice varieties under UV-B conditions

(Additional file 2: Table S3), ZS97 (Additional file 2: Table S4), Dular (Additional file 2: Table S5), and Lemon varieties (Additional file 2: Table S6), respectively, compared with the corresponding expression levels under the normal conditions (Fig. 2b). Among these DEGs, 1296 and 992 genes were commonly up-regulated and down-regulated by UV-B, respectively (Fig. 2c).

To gain insight into biological processes involved in the response to UV-B stress, Kyoto Encyclopedia of Genes and Genome (KEGG) pathway enrichment analysis was performed on the 2288 UV-B-responsive DEGs in these four rice varieties. The set of 1296 commonly up-regulated DEGs was mainly involved in phenylalanine, tyrosine, and tryptophan biosynthesis, phenylpropanoid metabolism, and flavonoid biosynthesis (Fig. 2d). The 992 DEGs uniquely down-regulated under UV-B stress were mostly enriched in glycine, serine, and threonine metabolism, glyoxylate and dicarboxylate metabolism, and cysteine and methionine metabolism (Fig. 2e). These results imply that the regulation of phenylpropanoid, tyrosine, and tryptophan biosynthesis plays crucial roles in the response to UV-B stress in rice, consistent with the metabolome profiling results under the UV-B conditions.

### Genetic basis of differential metabolites in response to UV-B in rice

To investigate the genetic basis of the differential metabolites identified in response to UV-B stress in rice seedlings, we calculated the coefficient of variation of 810 metabolites in the 160 rice varieties under normal and UV-B conditions. The results showed a higher proportion of variance in rice varieties under the UV-B conditions, implying that the metabolites responding under UV-B treatment exhibited significant genetic diversity (Additional file 1: Fig. S4). Subsequently, mGWAS was performed in the normal and UV-B conditions to identify significant loci associated with the differential metabolites (Fig. 3a, b; Additional file 1: Fig. S5). A total of 3127 and 4149 significantly induced loci were detected under normal and UV-B conditions, respectively, indicating their relevance for screening candidate genes to explore the genetic basis of differential metabolites in response to UV-B stress.

To explore the functions of genes associated with UV-B stress in these significant loci, Gene Ontology (GO) enrichment and KEGG pathway enrichment analyses were conducted. The majority of the candidate genes were involved in biological processes, cellular components, and molecular functions by GO analysis (Additional file 1: Fig. S6; Additional file 2: Table S7). Additionally, KEGG pathway analysis revealed that the genes that were induced under normal conditions were primarily involved in amino acid metabolism, fatty acid metabolism, and glycolysis, whereas those induced under the UV-B conditions were predominantly involved in phenylpropanoid biosynthesis, phenylalanine metabolism, and starch and sucrose metabolism (Additional file 1: Fig. S7; Additional file 2: Table S8). These analyses supported that the regulation of phenylpropanoid biosynthesis and phenylalanine metabolism likely play critical roles in the UV-B response and tolerance in rice. Combined with the results of the transcriptome data, candidate genes involved in amino acid and flavonoid metabolism were further determined and identified.

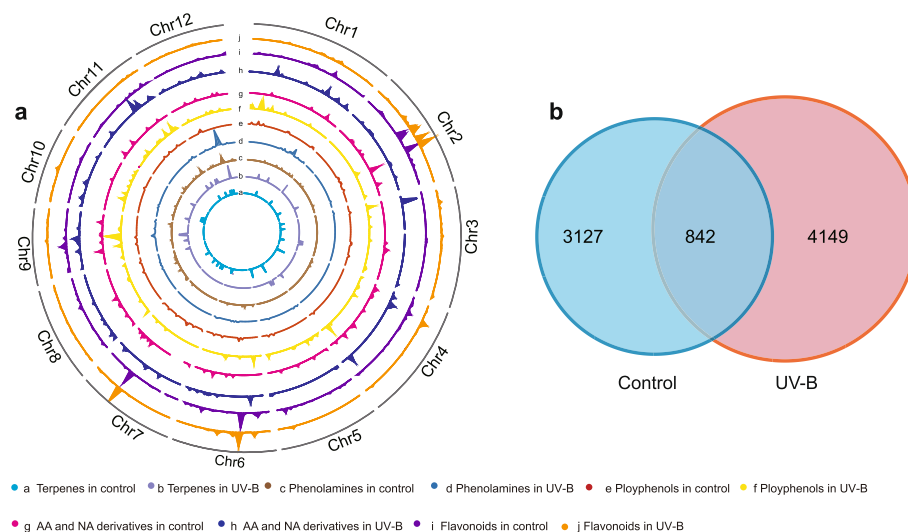


**Fig. 3** Overall mGWAS results of the metabolic features in rice seedling leaves under normal and UV-B conditions. **a** Genomic distribution of mGWAS results for the metabolic features in rice seedling leaves under normal and UV-B conditions; all metabolite–SNP associations with  $P \leq 5.0 \times 10^{-6}$  are plotted; metabolites were grouped into seven categories and marked with different colors namely a–e. **b** Venn diagram showing the number of significant loci in mGWAS result under normal and UV-B conditions;  $P \leq 5.0 \times 10^{-6}$



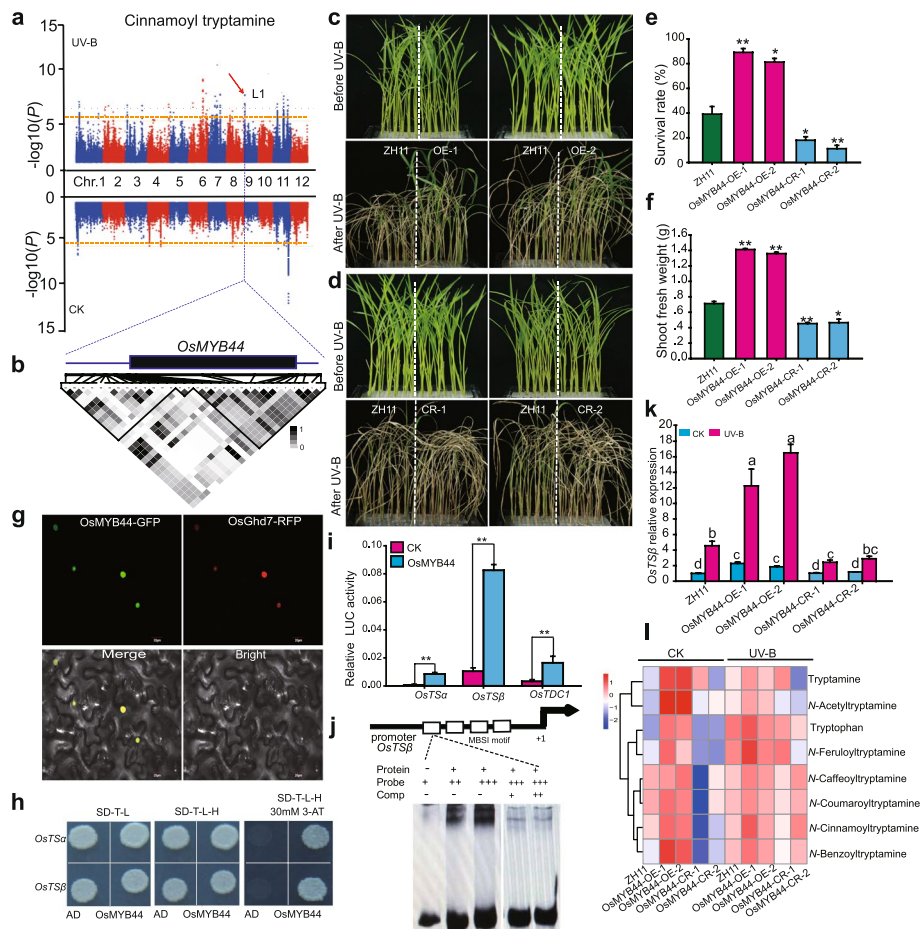


**Fig. 4** Identification and functional determination of *OsMYB44* in rice. **a** Manhattan plots showing the GWAS result on cinnamoyl tryptamine content in the leaves of 160 rice varieties in normal and UV-B conditions. **b** Association between polymorphic sites within the *OsMYB44* loci and cinnamoyl tryptamine content (each dot represents a polymorphic site); representation of pairwise  $r^2$  values (a measure of LD) among polymorphic sites in *OsMYB44*. **c, d** Phenotypes of 4-week-old *OsMYB44*-overexpressing (**c**) and *OsMYB44*-CRISPR (**d**) rice seedling lines and wild-type seedling lines before UV-B treatment and after 72 h UV-B treatment for 10-day recovery. **e** Survival rate of 4-week-old *OsMYB44* transgenic rice seedlings and wild-type seedlings after UV-B treatment for 10-day recovery. **f** Shoot fresh weight of *OsMYB44* transgenic rice seedlings and wild-type seedlings after UV-B treatment for 10-day recovery. **g** Subcellular localization of *OsMYB44* in tobacco leaves; *OsGhd7*-RFP used as a nuclear marker, bars 20  $\mu\text{m}$ . **h** Yeast-one hybrid assays showing the *OsMYB44* bound to *OsTSa* and *OsTS $\beta$*  promoter, an empty vector expressing the AD domain as the negative control. **i** Bar graphs showing the activity of the *ProOsTSa*:*LUC* reporter, the *ProOsTS $\beta$* :*LUC* reporter, and the *ProOsTDC1*:*LUC* reporter in tobacco leaves. LUC activity value was normalized to REN activity as an internal control; REN, renilla luciferase; LUC, firefly luciferase. **j** Electrophoretic mobility shift assay (EMSA) analysis of *OsMYB44* binding to the MBSI motif in the *OsTS $\beta$*  promoters. Fifty-fold molar excesses of unlabelled probes were used in the competition assay. **k** Relative expression levels of *OsTS $\beta$*  in *OsMYB44* transgenic rice seedling leaves and wild-type seedling leaves under normal and UV-B conditions by qRT-PCR. **l** Relative content of tryptamine and tryptamine derivatives in *OsMYB44* transgenic rice seedling lines under UV-B conditions. Data in **e, f, i**, and **k** are shown as the means  $\pm$  SD ( $n = 3$ ) and \*,  $P < 0.05$  and \*\*,  $P < 0.01$  (Student's *t*-test) indicate significant differences

### *OsMYB44* regulates tryptamine accumulation contributing to UV-B tolerance in rice

*N*-cinnamoyl tryptamine, a derivative of tryptamine, exhibited distinct loci under the UV-B stress conditions, as demonstrated by association analysis (Fig. 4a; Additional file 2: Table S9). Candidate gene selection revealed that locus L1, SNP 900647643

( $P=9.8 \times 10^{-9}$ ), was situated 7 kb upstream of *OsMYB44*, encoding a transcription factor in the MYB family (Fig. 4b; Additional file 1: Fig. S8). Moreover, induction analysis showed that UV-B significantly induced the expression of *OsMYB44* in rice, along with genes associated with tryptamine biosynthesis, namely *OsTS $\alpha$* , *OsTS $\beta$* , *OsTDC1*, *OsTDC3*, *OsTHT1*, and *OsTBT2* (Additional file 1: Fig. S9).

To confirm the function of *OsMYB44* in rice, we first analyzed its potential role in UV-B stress tolerance in *OsMYB44*-overexpressing and CRISPR-mediated *OsMYB44*-silenced rice seedling lines. The overexpression lines exhibited UV-B stress tolerance as evidenced by their green leaves under UV-B exposure (Fig. 4c, e). In contrast, the *OsMYB44*-CRISPR rice seedling lines showed clear withering symptoms and lower survival rates compared to those of wild-type seedlings after UV-B treatment (Fig. 4d, e). Consistent with these findings, the shoot fresh weight of the *OsMYB44*-overexpressing lines was higher than that of the wild type under UV-B exposure (Fig. 4f), indicating that *OsMYB44* positively regulates UV-B tolerance in rice.

Further examination of the mechanism underlying *OsMYB44*-mediated UV-B tolerance in rice revealed that *OsMYB44* as a functional transcription factor, directly binding to the promoters of *OsTS $\alpha$*  and *OsTS $\beta$*  (Fig. 4g, h) and significantly activating *ProOsTS $\alpha$ :LUC*, *ProOsTS $\beta$ :LUC*, and *ProOsTDC1:LUC* reporter activities (Fig. 4i). The electrophoretic mobility shift assay results further confirmed that *OsMYB44* directly binds to the MBSI element in the *OsTS $\beta$*  promoter (Fig. 4j). Moreover, the expression levels of *OsTS $\alpha$* , *OsTS $\beta$* , *OsTDC1*, and *OsTHT1* were significantly increased in *OsMYB44*-overexpressing seedling lines, particularly after UV-B treatment (Fig. 4k; Additional file 1: Fig. S10). Consequently, the contents of *N*-cinnamoyl tryptamine, *N*-benzoyl tryptamine, *N*-*p*-coumaroyl tryptamine, and tryptamine significantly increased in these lines (Fig. 4l). These results suggest that *OsMYB44* regulates tryptamine biosynthesis to enhance UV-B tolerance in rice. To further investigate the response of tryptamine to UV-B stress in rice, the rice seedlings were treated with exogenous tryptamine, resulting in a significant enhancement of their UV-B stress tolerance compared to that in the control conditions (Additional file 1: Fig. S11a–c). The survival rate of rice seedlings treated with tryptamine was considerably higher than that in the control conditions, especially after 48 h of UV-B exposure (Additional file 1: Fig. S11d). Therefore, we can conclude that *OsMYB44* promotes UV-B tolerance in rice by regulating tryptamine accumulation.

### **OsUVR8 interacts with OsMYB110 to regulate flavonoid accumulation contributing to UV-B tolerance in rice**

*C*-hexosyl-luteolin *O*-hexoside, a flavonoid derivative, displayed distinct genetic loci associated with UV-B stress, as revealed in the association analysis (Fig. 5a). Candidate gene selection identified locus L2, SNP421222223 ( $P=1.9 \times 10^{-10}$ ), on chromosome 4 positioned upstream of *OsUVR8*, which is a regulator encoding a protein with multiple RCC1 domains involved in chromosome condensation (Fig. 5b; Additional file 2: Table S10). Phylogenetic analysis demonstrated the similarity of UVR8 amino acid sequences between monocotyledons and dicotyledons (Fig. 5c). Co-expression analysis revealed significant enrichment of co-expressed genes with *OsUVR8* in flavonoid biosynthesis (Fig. 5d). Furthermore, the overexpression of *OsUVR8* in rice seedling lines led to the upregulation of *OsPAL1*, *OsACL5*, and *OsCHS* expression,



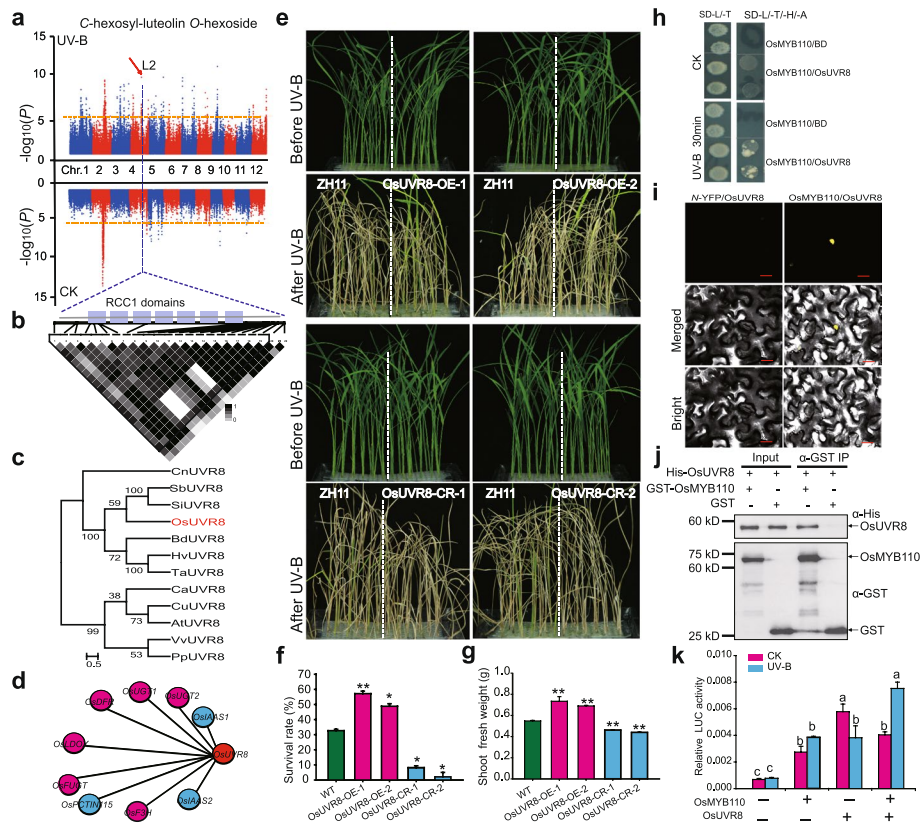


**Fig. 5** Identification and functional determination of *OsUVR8* and *OsMYB110* in rice. **a** Manhattan plots showing the GWAS result on C-hexosyl-luteolin O-hexoside content in the leaves of 160 rice varieties under normal and UV-B conditions. **b** Association between polymorphic sites within the *OsUVR8* loci and C-hexosyl-luteolin O-hexoside content (each dot represents a polymorphic site); representation of pairwise  $r^2$  values (a measure of LD) among polymorphic sites in *OsUVR8* containing many RCC1 domain. **c** Phylogenetic comparison of *OsUVR8* in plants; bootstrap values from 1000 resamplings are indicated. The bar represents 0.5 amino acid substitutions per site. **d** Co-expressed analysis of *OsUVR8* in rice. **e** Phenotypes of 4-week-old *OsUVR8* transgenic rice seedling lines and wild-type seedling lines before UV-B treatment and after 72 h UV-B treatment for 10-day recovery. **f** Survival rate of 4-week-old *OsUVR8* transgenic rice seedlings and wild-type seedlings after UV-B treatment for 10-day recovery. **g** Shoot fresh weight of *OsUVR8* transgenic rice seedlings and wild-type seedlings after UV-B treatment for 10-day recovery. **h** Yeast two-hybrid assay for interaction between *OsUVR8* and *OsMYB110*, empty vectors pGADT7 as a control in UV-B conditions. **i** BiFC analysis for interaction between *OsUVR8* and *OsMYB110* in tobacco, full-length *OsUVR8* fused to C-terminal YFP (*OsUVR8*-cYFP) and full-length *OsMYB110* fused to N-terminal YFP (nYFP-*OsMYB110*); *OsUVR8*-cYFP and nYFP as controls, bars 20  $\mu\text{m}$ . **j** In vitro pull-down assays showing *OsUVR8* interacting with *OsMYB110*. His-*OsUVR8* were incubated with GST-MYB110 and pulled down from GST-MYB110 conjugated GST beads. The eluates were analyzed by immunoblots with anti-His and anti-GST antibodies respectively. **k** Bar graphs showing the activity of *ProOsCHS:LUC* reporter in tobacco leaves. LUC activity value was normalized to REN activity as an internal control; REN, renilla luciferase; LUC, firefly luciferase. Data in **f**, **g**, and **k** are shown as the means  $\pm$  SD ( $n = 3$ ) and \*,  $P < 0.05$  and \*\*,  $P < 0.01$  (Student's *t*-test) indicate significant differences

while the downregulated expression of these genes was observed in *OsUVR8*-CRISPR rice seedling lines (Additional file 1: Fig. S12a–e). Accordingly, the content of several flavonoids such as methyl apigenin C-hexoside, C-hexoside-apigenin O-p-coumaroyl hexoside, chrysoeriol 7-O-rutinoside, and C-hexoside-chrysoeriol O-hexoside significantly increased in *OsUVR8*-overexpressing rice seedling lines (Additional file 1: Fig. S12f). These findings indicate that *OsUVR8* plays a regulatory role in flavonoid accumulation in rice. Additionally, the *OsUVR8*-overexpressing

rice seedling lines exhibited enhanced tolerance to UV-B stress, with notably higher survival rates, while *OsUVR8*-CRISPR rice seedling lines displayed increased sensitivity to UV-B stress, with lower survival rates compared to those of wild-type rice lines after UV-B treatment (Fig. 5e, f). Notably, the shoot fresh weight was higher in *OsUVR8*-overexpressing rice seedling lines compared to that of wild-type rice lines following UV-B treatment (Fig. 5g). These results indicated that *OsUVR8* is involved in flavonoid accumulation and UV-B tolerance in rice.

To investigate the role of *OsUVR8* in flavonoid accumulation and UV-B tolerance in rice, a yeast two-hybrid screen was conducted with and without UV-B treatment to identify proteins interacting with *OsUVR8*. *OsMYB110* was identified as an interacting partner in the presence of UV-B treatment (Fig. 5h). Bimolecular fluorescence complementation and GST pull-down assays further confirmed the interaction between *OsUVR8* and *OsMYB110* in vivo and in vitro (Fig. 5i, j). Moreover, transient transcription analysis demonstrated that both *OsUVR8* and *OsMYB110* individually activated the activity of *ProOsCHS:LUC*, with a more pronounced effect observed when *OsUVR8* was co-expressed with *OsMYB110*, particularly under the UV-B conditions (Fig. 5k).

To further underline the involvement of *OsMYB110* in flavonoid accumulation and UV-B tolerance in rice, the UV-B-induced expression patterns of *OsMYB110* and key genes involved in flavonoid biosynthesis, including *OsPAL1*, *Os4CL5*, *OsCHS*, *OsF3H*, *OsFLS*, and several *OsUGTs*, were analyzed, revealing significant upregulation under UV-B stress (Additional file 1: Fig. S13). Yeast one-hybrid and transient transcription assays demonstrated the binding of *OsMYB110* to the promoters of *OsPAL1*, *Os4CL5*, and *OsCHS*, along with remarkable activation of *ProOsPAL1:LUC*, *ProOs4CL5:LUC*, *ProOsC4H:LUC*, and *ProOsCHS:LUC* reporter activities (Additional file 1: Fig. S14a, b). Moreover, *OsPAL1*, *Os4CL5*, *OsCHS*, *OsF3H*, and *OsCGT* showed significant upregulation in *OsMYB110*-overexpressing rice seedling lines, particularly after UV-B treatment (Additional file 1: Fig. S14c). Consequently, higher levels of most flavonoids were observed in *OsMYB110*-overexpressing rice seedling lines under both normal and UV-B conditions (Additional file 1: Fig. S14d). Additionally, *OsMYB110*-overexpressing rice seedling lines exhibited reduced UV-B-induced damage and higher survival rates compared to those of the wild-type rice lines (Additional file 1: Fig. S14e, f). Similarly, the shoot fresh weight of *OsMYB110*-overexpressing rice seedling lines was significantly higher than that of the wild-type rice lines after UV-B treatment (Additional file 1: Fig. S14g). These findings provide evidence that *OsUVR8* interacts with *OsMYB110* to regulate flavonoid accumulation and enhance UV-B tolerance in rice.

### Natural variation of *OsUVR8* contributes to UV-B tolerance in rice

To investigate the relationship between *OsUVR8* haplotypes and UV-B intensity in a diverse collection of rice accessions in the world, the nucleotide polymorphisms of *OsUVR8* were analyzed in 4275 rice accessions based on information from RiceVarMap V2.0 (<http://ricevarmap.ncpgr.cn/>). Twenty-five SNPs and insertion-deletions were categorized into two distinct groups, namely group A and group B, which encompassed thirteen haplotypes. Group A consisted of haplotypes H3, H4, H5, H6, H7, and H10, and the remaining haplotypes were assigned to group B (Fig. 6a, b). Interestingly, rice varieties with haplotypes in group A (referred to as *OsUVR8*<sup>groupA</sup>) exhibited significantly

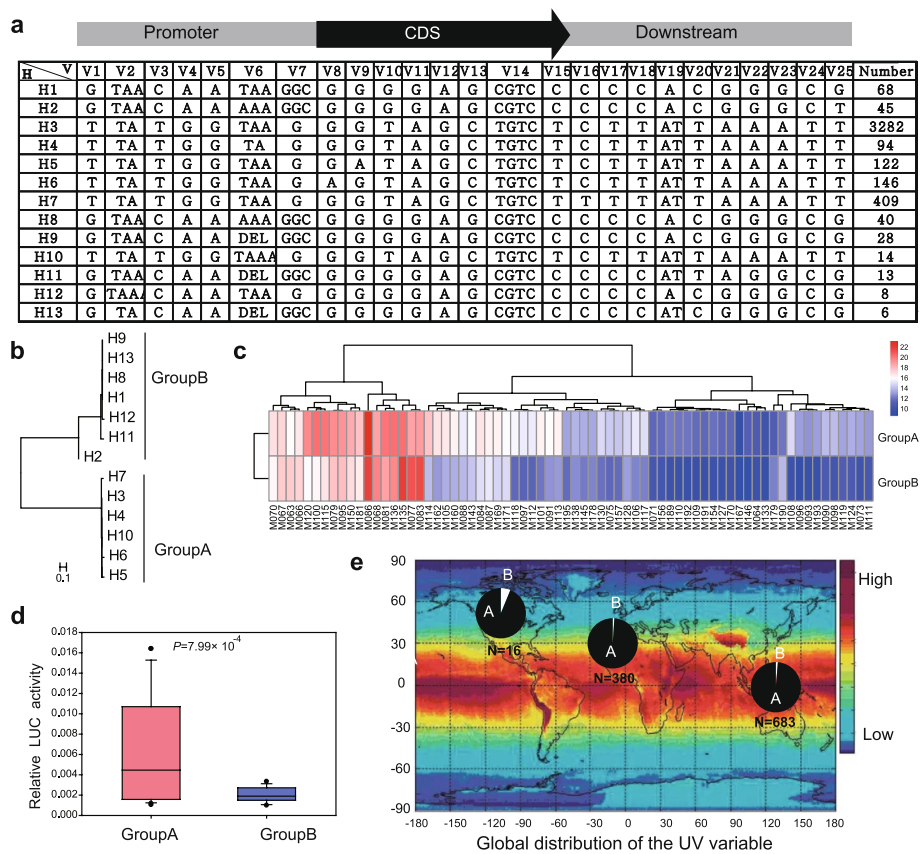


**Fig. 6** Natural variation and geographical distribution of *OsUVR8* in rice varieties. **a** Haplotype analysis of *OsUVR8* in 4275 rice varieties; thirteen haplotypes were detected, and the numbers of rice accessions with thirteen haplotypes were shown. **b** Phylogenetic tree of the thirteen haplotypes divided into group A (Hap3–Hap7 and Hap10), and group B (Hap1, Hap2, Hap8, Hap9, Hap11, Hap12, and Hap13). The scale bar indicates the average number of substitutions per site for different haplotypes. **c** Hierarchical clustering showing flavonoid accumulation in rice variety leaves with the two Groups. Red represents high flavonoid content, and blue represents low flavonoid content. **d** Bar graphs showing the promoter activity of the *OsUVR8* with different haplotypes in tobacco. LUC activity value was normalized to REN activity as an internal control; REN, renilla luciferase; LUC, firefly luciferase. **e** Geographic distribution among rice varieties with group A and group B in this study. Each pie chart size was proportional to the number of rice accessions with different groups in geographic location; red showing high UV-B intensity and blue showing low UV-B intensity

high levels of most flavonoids (61 upregulated patterns in 70 differentially accumulated flavonoids) with  $P < 0.05$ , whereas rice varieties with haplotypes in group B (referred to as *OsUVR8*<sup>groupB</sup>) displayed notably low levels of most flavonoids (Fig. 6c). Transient assays further revealed that the promoter activity of *OsUVR8*<sup>groupA</sup> was substantially higher than that of *OsUVR8*<sup>groupB</sup> in tobacco (Fig. 6d). Moreover, geographical distribution analysis demonstrated that approximately 6% of rice varieties with *OsUVR8*<sup>groupB</sup> and only 1% of varieties with *OsUVR8*<sup>groupB</sup> inhabit areas characterized by low and high UV-B intensity (Fig. 6e). These findings suggest that rice varieties with *OsUVR8*<sup>groupA</sup> are likely to have been artificially selected for their ability to withstand high UV-B intensity conditions.

## Discussion

In recent years, metabolomic analyses have become increasingly prominent in research concerning a variety of crops, including rice, maize, and foxtail millet [37, 38]. Despite significant advancements in this field, there is a paucity of studies delving into the biochemical and genetic underpinnings of the response of plant metabolomes to stress conditions. Our investigation focuses on the metabolomic responses of rice to UV-B radiation, utilizing an in-depth targeted metabolic profiling strategy. We discovered that a diverse set of flavonoids underwent significant reprogramming in response to UV-B stress, as shown in Fig. 1. This observation aligns with findings in Qingke barley reported by Zeng et al. (2020). Additionally, we observed an increase in the levels of several amino acids during UV-B exposure (Fig. 1). Interestingly, the difference of metabolite accumulation was more obvious between *indica* and *japonica* accessions under UV-B stress compared with normal conditions (Fig. 1a). Due to the differing geographic distributions of *indica* and *japonica* accession, these two subspecies encounter distinct environmental stresses. Flavonoids and amino acids have been reported to play roles in various abiotic stress responses and resistance [39, 40]. Therefore, we hypothesize that the specific accumulation of these metabolites may be significant both biologically and evolutionarily in the differentiation of *indica* and *japonica* accessions, as well as their adaptation to environmental stresses. Corroboratively, our transcriptomic analysis indicated that genes upregulated under UV-B conditions predominantly participate in the biosynthesis of specific amino acids (including phenylalanine, tyrosine, and tryptophan), phenylpropanoid metabolism, and flavonoid biosynthesis, echoing the alterations observed in the metabolome due to UV-B stress (Fig. 2). Intriguingly, genes with downregulated expression in response to UV-B were primarily related to the metabolism of glycine, serine, and threonine; the metabolism of glyoxylate and dicarboxylate; and the biosynthesis of cysteine and methionine (Fig. 2). These insights indicate that UV-B stress triggers extensive remodeling of various metabolic pathways, notably those of phenylpropanoids, flavonoids, and amino acids in rice. Consequently, it appears that metabolomic and transcriptomic responses to stress play a crucial role in the ability of plants to respond, tolerate, and adapt to environmental challenges.

With the rapid evolution of sequencing technologies, mGWAS have become increasingly powerful and efficient tools for elucidating the genetic determinants of metabolite profiles in a wide range of species [41]. Despite its potential, applications of mGWAS in exploring plant responses to adverse stress conditions remain relatively rare. In this study, we conducted a mGWAS to investigate the effects of UV-B stress on rice and identified numerous genetic loci significantly associated with metabolites responsive to UV-B exposure, such as amino acids, flavonoids, and polyphenols. These associations surpassed those detected under control conditions (Fig. 3; Additional file 1: Fig. S5). Therefore, our findings contribute a significant layer of understanding to the genetic architecture underlying UV-B-responsive metabolites in rice. Notably, our study pinpointed the transcription factor *OsMYB44* as a unique genetic locus identified through mGWAS based on its association with cinnamoyl tryptamine levels during UV-B stress. Further biochemical and genetic analyses confirmed that *OsMYB44* directly targets and activates the promoter of *OsTS $\beta$* , leading to increased *OsTS $\beta$*  expression and regulation of tryptamine biosynthesis in rice. Moreover, *OsMYB44* expression is induced

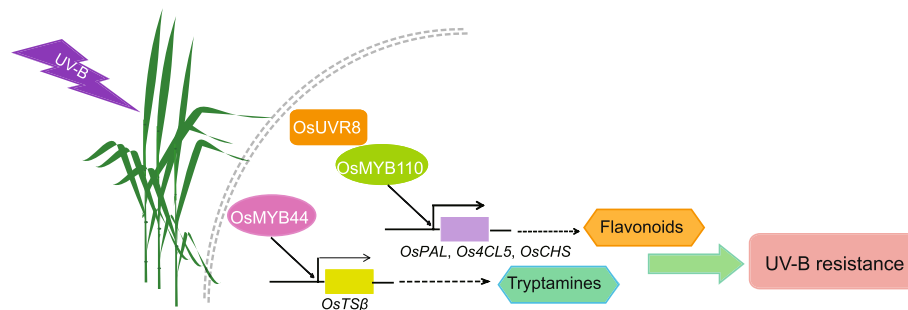


**Fig. 7** A proposed model of metabolomic-mediated UV-B resistance in rice

by UV-B stress, and rice seedlings overexpressing *OsMYB44* demonstrated enhanced tolerance to such stress (Fig. 4). Additionally, we identified and investigated the role of *OsMYB110*, revealing its interaction with the UV-B receptor *OsUVR8* (Fig. 5). Previous studies have documented that *OsMYB110* regulates the enzymes *OsPAL1*, *Os4CL3*, and *Os4CL5*, which are involved in lignin synthesis and resistance to brown planthoppers [36, 42]. In line with these previous findings, our observations suggest that *OsMYB110* interacts with the promoters of *OsPAL1*, *Os4CL5*, and *OsCHS* to boost their transcription, thereby promoting flavonoid accumulation under UV-B stress in rice and enhancing UV-B tolerance (Fig. 5; Additional file 1: Fig. S14). In conclusion, *OsMYB44* and *OsMYB110* emerged not only as key players in the UV-B stress response of rice but also hold promise as genetic resources to improve UV-B stress resistance in rice and potentially in other important crops such as wheat and maize (Fig. 7). Nevertheless, the naturally occurring alleles of *OsMYB44* and *OsMYB110* that impart UV-B tolerance are still largely uncharacterized and represent an exciting avenue for further research.

*AtUVR8*, the primary UV-B photoreceptor in *Arabidopsis*, has been extensively characterized based on its role in guiding plant responses to UV-B radiation [13]. Beyond this primary role, *AtUVR8* has been posited to participate in several additional physiological processes such as the regulation of stomatal opening [43], thermomorphogenic growth [44], and modulation of shade-avoidance responses [15]. In the present study, we uncovered that *OsUVR8*, the rice homolog of *AtUVR8*, contributes to the modulation of flavonoid synthesis (Additional file 1: Fig. S12), a finding that corresponds with previous studies [45–47]. Intriguingly, our data point to an interaction between *OsUVR8* and *OsMYB110* that collectively modulates the accumulation of flavonoids in rice (Fig. 5). A key discovery of our work was that *OsUVR8* plays an active role in promoting flavonoid accumulation to enhance UV-B stress tolerance, with natural variants within the *OsUVR8* locus, group A specifically, linked to heightened UV-B resistance in rice (Fig. 6), which were similar to natural variation of rice flavone accumulation and UV-tolerance reported previously [31]. These results collectively revealed the fact that, the natural variation of rice flavonoid accumulation is regulated not only by structural genes involved in flavonoid biosynthesis but also by certain upstream proteins, and exploring the naturally occurring allelic variations can provide a better understanding of gene function from physiological, ecological and evolutionary perspectives. Collectively, these results provide new insights for further studies of rice response, tolerance, and adaptation to



UV-B stress, and underscore the significance of *OsUVR8* as a valuable molecular breeding target for improving rice resilience and productivity under UV-B stress to ultimately bolster crop tolerance to environmental stressors.

## Conclusions

In summary, our investigation provides a comprehensive analysis of the metabolic and transcriptomic alterations in rice induced by UV-B radiation and pinpoints three genes integral to UV-B tolerance (Fig. 7). This study sheds light on the complex biochemical and genetic foundations that govern the metabolite dynamics underlying the response, tolerance, and adaptive strategies of rice to UV-B stress, utilizing cutting-edge genetic and molecular approaches. The insights gained from this research enrich our knowledge of the genetic strategies that underlie crop resilience, offering the potential to enhance agricultural sustainability by improving crop resistance to a spectrum of biotic and abiotic stresses.

## Methods

### Plant growth conditions and stress experiments

160 rice accessions were randomly selected for UV-B stress, which included 76 *Indica*, 58 *Japonica*, 3 *Admix*, 17 *Aus*, and 6 *VI*, based on the proportion of rice different subgroups in the 533 rice varieties from all over the world [28]. Information about these accessions, including the variety name and the place of origin, is listed in Additional file 2: Table S1. The 160 rice accessions were sown and grown in a growth pool in Huazhong Agricultural University, Wuhan. After 1 week, each variety was divided into two groups respectively and grown in two areas with equal conditions. Four weeks later, rice seedlings in one area were moved to a UV-B chamber (TL40W/302 nm narrowband UV-B tube, Philips, Netherlands) with  $30 \mu\text{W cm}^{-2}$  UV-B intensity. UV-B intensity was detected by a UV radiometer with the UV-295 detector from the photoelectric instrument factory (Beijing Normal University, China). And rice seedlings in the other area were grown in normal conditions. After UV-B treatment for 24 h, the fully expanded leaves of at least three lines from each variety in UV-B and normal conditions were harvested and snap-frozen in liquid nitrogen and stored at  $-80^\circ\text{C}$  for a metabolite sample, and every sample was repeated two times.

For transgenic rice seedlings with UV-B treatment, 4-week-old rice seedling leaves grown in normal conditions were transferred to a UV-B chamber (TL8W/302 nm narrowband UV-B tube, Philips, Netherlands) with  $12.8 \mu\text{W}$  UV-B intensity. When these rice seedlings were irradiated under UV-B conditions for 24 h, RNA and metabolite samples were obtained. When these rice seedlings were irradiated with UV-B for 72 h, these rice seedlings were moved into normal conditions to renew for 10 days. And then the surviving plants were counted.

### Metabolic profiling analysis

The metabolites were extracted and detected as previously described [35, 36]. In brief, the freeze-dried samples were crushed by a mixer mill (MM 400, Retsch) for 1.5 min at 30 Hz. 100 mg powder was weighed and extracted overnight at  $4^\circ\text{C}$  with 1.0 ml of 70%



aqueous methanol (methanol: H<sub>2</sub>O, 70:30, v/v). After the samples were centrifugated at 10,000 g for 10 min at 4 °C, the supernatants were collected, filtered (SCAA-104, 0.22 μm pore size; ANPEL, Shanghai, China) and detected by LC–MS.

Samples were detected by both LC-ESI-QTOF-MS/MS (TripleTOF 5600+, Applied Biosystems, USA) and LC-ESI-QTRAP-MS/MS (4000 QTRAP, Applied Biosystems, USA) for the MS<sup>2</sup> spectral tag (MS2T) library construction. In the TOF MS mode, the scanning mass range was from m/z 100 to m/z 1000 with an accumulation time of 0.10 s. For IDA, the CEs were set at 30 V and 50 V, survey scans were acquired in 0.08 s, and as many as 10 product ion scans were collected. The total cycle time was fixed to 0.79 s. In the stepwise scan MIM–EPI mode, the Q1 (Q3) was set from 100.1 to 1000.1 Da, and the mass step was 1.0 Da, such as from 100.1/100.1, 101.1/101.1, 102.1/102.1, to 1000.1/1000.1. Each MIM transition was performed with a 5-ms Dwell time, and each MIM–EPI experiment with 60 MIM transitions monitored [35].

As described previously, a scheduled multiple reaction monitoring (MRM) method was used to carry out the quantification of the metabolites [35]. An MRM detection window of 90 s and a target scan time of 1.0 s were used in the scheduled MRM algorithm. The data were processed with Analyst 1.6 software.

### Metabolite data analysis

Metabolite data were the first log<sub>2</sub> transformed to improve the normality of distribution. PCA was performed using *R* ([www.r-project.org/](http://www.r-project.org/)) software with default settings. Z-score was used for the normalization of metabolite content, and then PCA analysis was performed. The significantly changed ( $P < 0.05$ , |Fold Change| ≥ 5) metabolites were used for comparison analysis between UV-B treatment and normal conditions. Differences in the metabolites of rice leaves between treatment and normal conditions were determined using unpaired two-tailed Student's *t*-tests ( $P < 0.05$ ). The fold change was calculated by comparing the ratio of average metabolite contents in 160 rice varieties under UV-B treatment and normal conditions.

The values of the CV were calculated independently for each metabolite (using the mean of the biological replicates of the untransformed m-trait data) as follows:  $s/m$ , where *s* and *m* are the SD and mean of each metabolite in the population, respectively [28].

### Genome-wide association analysis

Genome-wide association analysis (GWAS) was made in rice varieties in normal and UV-B conditions as described previously. In brief, SNP information was downloaded via the website RiceVarMap (<http://ricevarmap.ncpgr.cn>) [48]. Only SNPs with an MAF ≥ 0.05 and numbers of varieties with a minor allele ≥ 6 in a panel were used to perform GWAS. Population structure was modeled with a linear mixed model (LMM), where each SNP and Q matrix are taken as fixed factors for regression analysis, kinship is taken as a random factor for SNP significance test, *p*-value is the *p*-value of GWAS analysis, effect is the effect value of SNP [49, 50]. mGWAS was carried out based on LMM via the factored spectrally transformed LMM (FaST-LMM) program according to threshold value  $P = 6.9 \times 10^{-6}$ , respectively [51].

### Transgene constructions and transformations

*OsMYB44* (LOC\_Os09g01960), *OsMYB110* (LOC\_Os10g33810) and *OsUVR8* (LOC\_Os04g35570) overexpression vectors were constructed via directly inserting the full cDNAs into the entry vector pDONR207 and then into the destination vector PJC034 (vector pH2GW7 for overexpression with the maize ubiquitin promoter) as described previously [52]. *OsMYB44* and *OsUVR8* mutants were generated by the CRISPR-Cas9 method as previously described [53]. These vectors were introduced into *Agrobacterium tumefaciens* EHA105 and then were transformed into ZH11 by an agrobacterium-mediated transformation.

### Phylogenetic analysis

The amino acid sequences of reported genes including MYB transcription factors and UVR8s were obtained from NCBI (<http://www.ncbi.nlm.nih.gov/>). The amino acid sequences of *OsMYB44* and *OsUVR8* were gained from the Rice Genome Annotation Project (<http://rice.plantbiology.msu.edu/>). The alignment of amino acid sequences was carried out by ClustalW, and neighbor-joining trees were made via MEGA5. The reliability of the reconstructed phylogenetic tree was evaluated by a bootstrap test with 1000 replicates.

### Subcellular localization assays

The full-length coding sequences of *OsMYB44* were amplified and cloned into the pH7WG vector to generate an *OsMYB44*-GFP fusion construct driven by the constitutive cauliflower mosaic virus promoters (35S:*OsMYB44*-GFP and 35S:*OsGhd7*-RFP) as a nucleus marker were transiently expressed in tobacco (*Nicotiana benthamiana*) leaves via *A. tumefaciens*-mediated infiltration as described previously [54]. After 2 days, the fluorescence signals of *OsMYB44*-GFP, and *OsGhd7*-RFP fusion proteins in tobacco were observed by confocal laser scanning microscopy (Olympus FV1000, Olympus, Japan).

### Electrophoretic mobility shift assay (EMSA)

The vector of *OsMYB44* with His-tag was transformed and expressed in *E. coli* BL21 (DE3) and purified as described previously [31]. The 50 bp probes containing the MBSI motif of *OsMYB44* promoter with FAM as forwards and reverse strands were synthesized. *OsMYB44*-His-tag purifying protein (200–800 ng) was incubated in a 20- $\mu$ l reaction system (50 mmol/L sodium chloride, 1 mmol L<sup>-1</sup> EDTA, 1 mmol L<sup>-1</sup> dithiothreitol, 0.05 mmol L<sup>-1</sup> poly (deoxyinosinide oxycytidylic) sodium salt, and 10% glycerol) at room temperature (25 °C) for 10 min and then added to the FAM-labeled DNA (2 nmol L<sup>-1</sup>) at room temperature for 30 min. For competition assays, 50  $\times$  unlabeled probes containing MBSI motif and mutants were also added to the reactions. The reaction mixture was electrophoresed at 4 °C on a 6% native polyacrylamide gel in 0.5  $\times$  Tris–borate-EDTA for 1.5 h at 120 V. DNA gels were detected with TYPhoon 9410 (Amersham, England).

### Dual-luciferase reporter assay

The promoter fragments of *OsTS $\alpha$* , *OsTS $\beta$* , *OsTDC1*, *OsPAL1*, *Os4CL5*, *OsC4H*, and *OsCHS* were amplified and cloned into the pH2GW7 vector with the firefly luciferase (fLUC) gene and the renilla luciferase (rLUC) gene as reporters. Meanwhile, the full-length coding sequences of *OsMYB44*, *OsMYB110*, and *OsUVR8* were cloned into the pEAQ-HTDEST2 vector as effects. These vectors were transferred into *Agrobacterium* strain EHA105 and transiently expressed in tobacco leaves. The luciferase activities were measured by the dual luciferase reporter assay system (Promega, Madison, USA) based on the manufacturer's instructions. The luciferase activities were calculated by the ratio of fLUC to rLUC (LUC/REN).

### Yeast one-hybrid (Y1H) and yeast two-hybrid (Y2H) assays

Yeast one-hybrid assay was performed according to the Yeast Protocols Handbook (TaKaRa Bio, Japan). The respective combinations of AD fusion and pHIS2 vector were co-transformed into yeast strain AH109, grown on SD/-Leu-His medium, and then selected on SD/-His/-Leu/-Trp medium with 3-AT (3-amino-1,2,4-triazole). Yeast two-hybrid assays were carried out via the Matchmaker GAL4 Two-Hybrid System (BD Clontech). The respective combinations of pGADT7 and pGBKT7 fusion vectors were co-transformed into yeast strain AH109. The respective combinations of pGADT7 and empty pGBKT7 were co-transformed as a negative control. And then the transformed yeast cells were selected and cultivated on SD/-His/-Leu/-Trp/-Ade medium for 3 d at 30 °C.

### Bimolecular fluorescence complementation (BiFC) assay

The full-length coding sequences of *OsUVR8* and *OsMYB110* were amplified and then cloned into the nYFP and cYFP vectors to generate OsUVR8-nYFP, OsUVR8-cYFP, OsMYB110-nYFP, and OsMYB110-cYFP fusion vectors. OsUVR8-nYFP, OsUVR8-cYFP, OsMYB110-nYFP, and OsMYB110-cYFP vectors were transiently co-transformed into tobacco leaves via *A. tumefaciens*-mediated infiltration. The YFP signal was visualized by confocal laser scanning microscopy (Olympus FV1000, Olympus, Japan).

### In vitro GST pull-down assays

Full-length coding sequences of *OsUVR8* and *OsMYB110* were amplified and cloned into pET28a and pGEX-6P-1 vectors respectively. The recombinant vectors were transformed into *E. coli* strain BL21 (DE3) to express His-OsUVR8 and GST-OsMYB110 proteins. Recombinant His-OsUVR8 was incubated with GST-OsMYB110 and immobilized on GST beads (Cytiva 17075605). After being pulled down from GST beads, the proteins were subsequently analyzed by immunoblotting using anti-His antibody (Abclonal AE003, 1:10,000 dilution) to detect OsUVR8 and anti-GST antibody (Abclonal AE077, 1:5000 dilution) to detect OsMYB110. The GST proteins expressed from empty pGEX-6P-1 vector were incubated with His-OsUVR8 as a negative control.

### RNA sequencing and transcriptome analysis

Three-week-old rice seedling leaves from ZH11, ZS97, Dular, and Lemon were used for RNA sequencing as described previously [55]. Raw reads of each sample were generated and sequenced by an Illumina Hi Step 4000 (200 bp paired-end reads). The clean reads were obtained by removing the adapter, the unknown bases, and the low-quality sequence. High-quality reads were obtained by mapping to reference genome cultivar, Nipponbare with HISAT2. The gene expression levels were measured by transcripts per million (TPM). Differentially expressed genes (DEGs) were determined via the Benjamini–Hochberg FDR multiple testing correction with  $P$ -value  $< 0.05$ ,  $|\text{Fold Change}| > 2$  or  $|\text{Fold Change}| < 0.5$ .

### RNA extraction and qRT-PCR analysis

Rice total RNA was extracted with the TRIzol reagent kit (Invitrogen, Waltham, USA) according to the manufacturer's instructions. The first-strand cDNA was synthesized using the one-step gDNA removal and cDNA synthesis supermix (TransGen Biotech, Beijing, China) based on the manufacturer's instructions. qRT-PCR was performed using the SYBR Premix Ex Taq kit (TaKaRa Bio) on the ABI7500 Real-time PCR system (Applied Biosystems, USA). The rice reference gene was the UBIQUITIN gene (OsUBQ). Every gene was made three times, and the experiments were repeated twice. Gene-specific primers were designed by Primer Premier 5.0, and primer sequences were listed in Additional file 2: Table S11.

### Exogenous tryptamine treatment

Exogenous tryptamine treatment was carried out with 4-week-old rice ZH11 seedlings. In detail, ZH11 seeds were selected, sown, and grown in a normal conditions. After 3 weeks, 50 mM tryptamine dissolved in ethanol solution was sprayed onto the leaves of the rice seedlings, and the control rice seedlings were sprayed with ethanol solution. Then the rice seedlings were treated with UV-B stress for 72 h, moved into normal conditions to renew for 10 days, and then the surviving plants were counted.

### Supplementary Information

The online version contains supplementary material available at <https://doi.org/10.1186/s13059-024-03372-x>.

**Additional file 1:** Supplementary Figures. Fig. S1 Classes of 810 metabolites detected in this study. Fig. S2 Heatmap visualization of differential metabolites identified under UV-B condition compared to those under the normal condition. Fig. S3 Tolerance of different rice varieties to UV-B stress. Fig. S4 Distribution of coefficient of variation (CV) among the 160 rice accessions in normal condition and UV-B condition. Fig. S5 Manhattan plots showing the GWAS results of partial metabolites in normal and UV-B conditions. Red arrows showed new significant loci in manhattan plots under normal and UV-B conditions. Fig. S6 Gene ontology (GO) functional classifications and numbers of genes in significant loci on mGWAS results. Fig. S7 KEGG pathway enrichment analysis for genes in loci on mGWAS results ( $P \leq 5.0 \times 10^{-6}$ ) in normal condition (a) and UV-B condition (b). Fig. S8 Phylogenetic comparison of OsMYB44 and AtMYBs in Arabidopsis; bootstrap values from 1000 resamplings are indicated. The bar represents 0.5 amino acid substitutions per site. Fig. S9 Tryptamine biosynthetic pathway in plants (a) and induced expression profile of genes involved in tryptamine biosynthetic pathway by UV-B (b). Fig. S10 Relative expression levels of genes involved in tryptamine biosynthetic pathway in OsMYB44 transgenic rice seedling leaves. Fig. S11 Tolerance of rice seedling lines to UV-B stress under exogenous tryptamine treatment. Fig. S12 OsUVR8 involved in flavonoid accumulation in rice. Fig. S13 General flavonoid biosynthetic pathway in plants (a) and induced expression profile of genes involved in flavonoid biosynthetic pathway by UV-B stress (b). Fig. S14 OsMYB110 involved in flavonoid metabolism in rice.

**Additional file 2:** Supplementary Tables. Table S1 The list of collected 160 rice accessions in this study. Table S2 The information of metabolites determined in rice. Table S3 Transcriptome in ZH11 under UV-B stress. Table S4 Transcriptome in ZS97 under UV-B stress. Table S5 Transcriptome in Dular under UV-B stress. Table S6 Transcriptome in Lemon under UV-B stress. Table S7 Genes in significant loci on mGWAS results in normal condition. Table S8 Genes in

significant loci on mGWAS results in UV-B condition. Table S9 The prominent Indels and SNPs of OsMYB44 relevant to N-cinnamoyl tryptamine content. Table S10 The prominent Indels and SNPs of OsUVR8 relevant to C-hexosyl-luteolin O-hexoside content. Table S11 Primers used in this study.

**Additional file 3.** Uncropped images for the blots.

**Additional file 4.** Review history.

### Peer review information

Wenjing She was the primary editor of this article and managed its editorial process and peer review in collaboration with the rest of the editorial team.

### Review history

The review history is available as Additional file 4.

### Authors' contributions

F.Z., W.C., S.W., J.L., J.Y., and Y.L. designed the research and supervised this study. F.Z., S.S., Q.Z., C.L., C.W., T.Z., C.Z., L.Q., and X.L. participated in the material preparation. C.Y. and Y.L. carried out the metabolite analyses. F.Z., C.Y., and H.G. performed the data analyses. F.Z., J.Y., and Y.L. performed most of the experiments. F.Z., J.Y., C.Y., and Y.L. wrote the manuscript.

### Funding

This work was supported by the National Science Foundation of China (32101662, 32202248, and 32200218).

### Availability of data and materials

Transcriptome sequencing reads of the rice leaves of four rice varieties under UV-B and control conditions were deposited into the NCBI BioProject under the accession numbers PRJNA1123160 [56]. Metabolomics data in this paper have been deposited in the OMIX, China National Center for Bioinformatics / Beijing Institute of Genomics, Chinese Academy of Sciences (<https://ngdc.cncb.ac.cn/omix>) under the accession number OMIX006966 [57]. The source codes used for data analysis in this study were deposited under GPL-3.0 license in Github ([https://github.com/lyy-github668/Rice\\_RNAseq\\_mGWAS](https://github.com/lyy-github668/Rice_RNAseq_mGWAS)) [58] and Zenodo (<https://zenodo.org/records/12805102>) [59]. The rice reference genome was accessed from the Rice Genome Annotation Project (<http://rice.uga.edu/index.shtml>) [60]. The rice genotyping information was accessed from Rice Variation Map v2.0 (<https://ricevarmap.ncpgr.cn/>) [61]. The global distribution of the UV intensity was accessed from literature previously published [62]. The rice accession information was accessed from literature previously published [63, 64]. No other scripts and software were used other than those mentioned in the Methods section.

### Declarations

#### Ethics approval and consent to participate

Not applicable.

#### Consent for publication

Not applicable.

#### Competing interests

The authors declare that they have no competing interests.

Received: 16 January 2024 Accepted: 18 August 2024

Published online: 29 August 2024

### References

1. Wargent JJ, Jordan BR. From ozone depletion to agriculture: understanding the role of UV radiation in sustainable crop production. *New Phytol.* 2013;197(4):1058–76.
2. Bais AF, Bernhard G, McKenzie RL, Aucamp PJ, Young PJ, Ilyas M, et al. Ozone-climate interactions and effects on solar ultraviolet radiation. *Photochem Photobiol Sci.* 2019;18(3):602–40.
3. McKenzie RL, Aucamp PJ, Bais AF, Björn LO, Ilyas M, Madronich S. Ozone depletion and climate change: impacts on UV radiation. *Photochem Photobiol Sci.* 2011;10(2):182–98.
4. Kelbch A, Wittlich M, Bott A. Quantifying the effects of a low-ozone event and shallow stratocumulus clouds on ultraviolet erythemal radiation exposure. *Int J Biometeorol.* 2019;63(3):359–69.
5. Nawkar GM, Maibam P, Park JH, Sahi VP, Lee SY, Kang CH. UV-induced cell death in plants. *Int J Mol Sci.* 2013;14(1):1608–28.
6. Chu R, Zhang QH, Wei YZ. Effect of enhanced UV-B radiation on growth and photosynthetic physiology of *Iris tectorum maxim.* *Photosynth Res.* 2022;153(3):177–89.
7. Hader DP. Effects of solar UV-B radiation on aquatic ecosystems. *Adv Space Res.* 2000;26(12):2029–40.
8. Dhanya Thomas TT, Dinakar C, Puthur JT. Effect of UV-B priming on the abiotic stress tolerance of stress-sensitive rice seedlings: Priming imprints and cross-tolerance. *Plant Physiol Biochem.* 2020;147:21–30.
9. Jenkins GI. Signal transduction in responses to UV-B radiation. *Annu Rev Plant Biol.* 2009;60:407–31.

10. Shi C, Liu H. How plants protect themselves from ultraviolet-B radiation stress. *Plant Physiol.* 2021;187(3):1096–103.
11. Tossi VE, Regalado JJ, Iannicelli J, Laino LE, Burrieza HP, Escandón AS, et al. Beyond Arabidopsis: differential UV-B response mediated by UVR8 in diverse species. *Front Plant Sci.* 2019;10:780.
12. Fang F, Lin L, Zhang Q, Lu M, Skvortsova MY, Podolec R, et al. Mechanisms of UV-B light-induced photoreceptor UVR8 nuclear localization dynamics. *New Phytol.* 2022;236(5):1824–37.
13. Podolec R, Demarsy E, Ulm R. Perception and signaling of ultraviolet-B radiation in plants. *Annu Rev Plant Biol.* 2021;72:793–822.
14. Zedek F, Veselý P, Tichý L, Elliott TL, Garbolino E, de Ruffray P, et al. Holocentric plants are more competitive under higher UV-B doses. *New Phytol.* 2022;233(1):15–21.
15. Takshak S, Agrawal SB. Defense potential of secondary metabolites in medicinal plants under UV-B stress. *J Photochem Photobiol B.* 2019;193:51–88.
16. Jan R, Khan MA, Asaf S, Lubna, Waqas M, Park JR, et al. Drought and UV radiation stress tolerance in rice is improved by overaccumulation of non-enzymatic antioxidant flavonoids. *Antioxidants (Basel).* 2022;11(5):917.
17. Köhler H, Contreras RA, Pizarro M, Cortés-Antiquera R, Zúñiga GE. Antioxidant responses induced by UVB radiation in *Deschampsia antarctica* Desv. *Front Plant Sci.* 2017;8:921.
18. Del-Castillo-Alonso MÁ, Monforte L, Tomás-Las-Heras R, Ranieri A, Castagna A, Martínez-Abaigar J, et al. Secondary metabolites and related genes in *Vitis vinifera* L. cv. *Tempranillo* grapes as influenced by ultraviolet radiation and berry development. *Physiol Plant.* 2021;173(3):709–24.
19. Wang Y, Liu S, Wang H, Zhang Y, Li W, Liu J, et al. Identification of the regulatory genes of UV-B-induced anthocyanin biosynthesis in pepper fruit. *Int J Mol Sci.* 2022;23(4):1960.
20. Kusano M, Tohge T, Fukushima A, Kobayashi M, Hayashi N, Otsuki H, et al. Metabolomics reveals comprehensive reprogramming involving two independent metabolic responses of Arabidopsis to UV-B light. *Plant J.* 2011;67(2):354–69.
21. Gil M, Pontin M, Berli F, Bottini R, Piccoli P. Metabolism of terpenes in the response of grape (*Vitis vinifera* L.) leaf tissues to UV-B radiation. *Phytochemistry.* 2012;77:89–98.
22. Sun Q, Liu M, Cao K, Xu H, Zhou X. UV-B irradiation to amino acids and carbohydrate metabolism in *Rhododendron chrysanthum* leaves by coupling deep transcriptome and metabolome analysis. *Plants (Basel).* 2022;11(20):2730.
23. Fernie AR, Tohge T. The genetics of plant metabolism. *Annu Rev Genet.* 2017;51:287–310.
24. Fang C, Luo J. Metabolic GWAS-based dissection of genetic bases underlying the diversity of plant metabolism. *Plant J.* 2019;97(1):91–100.
25. Zhao K, Rhee SY. Omics-guided metabolic pathway discovery in plants: Resources, approaches, and opportunities. *Curr Opin Plant Biol.* 2022;67:102222.
26. Han B, Huang X. Sequencing-based genome-wide association study in rice. *Curr Opin Plant Biol.* 2013;16(2):133–8.
27. Dmitriev AA, Pushkova EN, Melnikova NV. Plant genome sequencing: modern technologies and novel opportunities for breeding. *Mol Biol (Mosk).* 2022;56(4):531–45.
28. Chen W, Gao Y, Xie W, Gong L, Lu K, Wang W, et al. Genome-wide association analyses provide genetic and biochemical insights into natural variation in rice metabolism. *Nat Genet.* 2014;46(7):714–21.
29. Chen J, Hu X, Shi T, Yin H, Sun D, Hao Y, et al. Metabolite-based genome-wide association study enables dissection of the flavonoid decoration pathway of wheat kernels. *Plant Biotechnol J.* 2020;18(8):1722–35.
30. Zhu F, Bulut M, Cheng Y, Alseekh S, Fernie AR. Metabolite-based genome-wide association studies of large-scale metabolome analysis to illustrate alterations in the metabolite landscape of plants upon responses to stresses. *Methods Mol Biol.* 2023;2642:241–55.
31. Peng M, Shahzad R, Gul A, Subthain H, Shen S, Lei L, et al. Differentially evolved glucosyltransferases determine natural variation of rice flavone accumulation and UV-tolerance. *Nat Commun.* 2017;8(1):1975.
32. Wu S, Tohge T, Cuadros-Inostroza Á, Tong H, Tenenboim H, Kooke R, et al. Mapping the Arabidopsis metabolic landscape by untargeted Metabolomics at different environmental conditions. *Mol Plant.* 2018;11(1):118–34.
33. Zeng X, Yuan H, Dong X, Peng M, Jing X, Xu Q, et al. Genome-wide dissection of co-selected UV-B responsive pathways in the UV-B adaptation of qingke. *Mol Plant.* 2020;13(1):112–27.
34. Zhao M, Lin Y, Chen H. Improving nutritional quality of rice for human health. *Theor Appl Genet.* 2020;133(5):1397–413.
35. Chen W, Gong L, Guo Z, Wang W, Zhang H, Liu X, et al. A novel integrated method for large-scale detection, identification, and quantification of widely targeted metabolites: application in the study of rice metabolomics. *Mol Plant.* 2013;6(6):1769–80.
36. Yang C, Shen S, Zhou S, Li Y, Mao Y, Zhou J, et al. Rice metabolic regulatory network spanning the entire life cycle. *Mol Plant.* 2022;15(2):258–75.
37. Scossa F, Brotman Y, de Abreu E Lima F, Willmitzer L, Nikoloski Z, Tohge T, et al. Genomics-based strategies for the use of natural variation in the improvement of crop metabolism. *Plant Sci.* 2016;242:47–64.
38. Li X, Gao J, Song J, Guo K, Hou S, Wang X, et al. Multi-omics analyses of 398 foxtail millet accessions reveal genomic regions associated with domestication, metabolite traits, and anti-inflammatory effects. *Mol Plant.* 2022;15(8):1367.
39. Tohge T, Wendenburg R, Ishihara H, Nakabayashi R, Watanabe M, Sulpice R, et al. Characterization of a recently evolved flavonol-phenylacyltransferase gene provides signatures of natural light selection in Brassicaceae. *Nat Commun.* 2016;7:12399.
40. Zhang F, Wu J, Sade N, Wu S, Egbaria A, Fernie AR, et al. Genomic basis underlying the metabolome-mediated drought adaptation of maize. *Genome Biol.* 2021;22(1):260.
41. Luo J. Metabolite-based genome-wide association studies in plants. *Curr Opin Plant Biol.* 2015;24:31–8.
42. He J, Liu Y, Yuan D, Duan M, Liu Y, Shen Z, et al. An R2R3 MYB transcription factor confers brown planthopper resistance by regulating the phenylalanine ammonia-lyase pathway in rice. *Proc Natl Acad Sci U S A.* 2020;117(1):271–7.
43. Tossi V, Lamattina L, Jenkins GI, Cassia RO. Ultraviolet-B-induced stomatal closure in Arabidopsis is regulated by the UV RESISTANCE LOCUS8 photoreceptor in a nitric oxide-dependent mechanism. *Plant Physiol.* 2014;164(4):2220–30.
44. Hayes S, Sharma A, Fraser DP, Trevisan M, Cragg-Barber CK, Tavidou E, et al. UV-B perceived by the UVR8 photoreceptor inhibits plant thermomorphogenesis. *Curr Biol.* 2017;27(1):120–7.



45. Liu L, Gregan S, Winefield C, Jordan B. From *UVR8* to flavonol synthase: UV-B-induced gene expression in *Sauvignon blanc* grape berry. *Plant Cell Environ*. 2015;38(5):905–19.
46. Clayton WA, Albert NW, Thrimawithana AH, McGhie TK, Derolles SC, Schwinn KE, et al. UVR8-mediated induction of flavonoid biosynthesis for UVB tolerance is conserved between the liverwort *Marchantia polymorpha* and flowering plants. *Plant J*. 2018;96(3):503–17.
47. Shamala LF, Zhou HC, Han ZX, Wei S. UV-B induces distinct transcriptional re-programing in UVR8-Signal transduction, flavonoid, and terpenoids pathways in *Camellia sinensis*. *Front Plant Sci*. 2020;11:234.
48. Zhao H, Yao W, Ouyang Y, Yang W, Wang G, Lian X, et al. RiceVarMap: a comprehensive database of rice genomic variations. *Nucleic Acids Res*. 2015;43(Database issue):1018–22.
49. Price AL, Zaitlen NA, Reich D, Patterson N. New approaches to population stratification in genome-wide association studies. *Nat Rev Genet*. 2010;11(7):459–63.
50. Zhang F, Guo H, Huang J, Yang C, Li Y, Wang X, et al. A UV-B-responsive glycosyltransferase, *OsUGT706C2*, modulates flavonoid metabolism in rice. *Sci China Life Sci*. 2020;63(7):1037–52.
51. Lippert C, Listgarten J, Liu Y, Kadie CM, Davidson RI, Heckerman D. FaST linear mixed models for genome-wide association studies. *Nat Methods*. 2011;8(10):833–5.
52. Zhang F, Huang J, Guo H, Yang C, Li Y, Shen S, et al. *OsRLCK160* contributes to flavonoid accumulation and UV-B tolerance by regulating *OsZIP48* in rice. *Sci China Life Sci*. 2022;65(7):1380–94.
53. Sun Y, Shi Y, Liu G, Yao F, Zhang Y, Yang C, et al. Natural variation in the *OsZIP18* promoter contributes to branched-chain amino acid levels in rice. *New Phytol*. 2020;228(5):1548–58.
54. Zhang Y, Chen K, Zhao FJ, Sun C, Jin C, Shi Y, et al. OsATX1 interacts with heavy metal P1B-Type ATPases and affects copper transport and distribution. *Plant Physiol*. 2018;178(1):329–44.
55. Zhang Z, Zhang F, Deng Y, Sun L, Mao M, Chen R, et al. Integrated metabolomics and transcriptomics analyses reveal the metabolic differences and molecular basis of nutritional quality in landraces and cultivated rice. *Metabolites*. 2022;12(5):384.
56. Zhang F, Yang C, Guo H, Li Y, Shen S, Qianqian Zhou Q, et al. Dissecting the genetic basis of UV-B responsive metabolites in rice. Datasets. Sequence Read Archive. <https://www.ncbi.nlm.nih.gov/bioproject/PRJNA1123160> (2024).
57. Zhang F, Yang C, Guo H, Li Y, Shen S, Qianqian Zhou Q, et al. Dissecting the genetic basis of UV-B responsive metabolites in rice. Datasets. OMIX. <https://ngdc.cncb.ac.cn/omix/release/OMIX006966> (2024).
58. Zhang F, Yang C, Guo H, Li Y, Shen S, Qianqian Zhou Q, et al. Dissecting the genetic basis of UV-B responsive metabolites in rice. Github. [https://github.com/lyy-github668/Rice\\_RNAseq\\_mGWAS](https://github.com/lyy-github668/Rice_RNAseq_mGWAS) (2024).
59. Zhang F, Yang C, Guo H, Li Y, Shen S, Qianqian Zhou Q, et al. Dissecting the genetic basis of UV-B responsive metabolites in rice. Zenodo. <https://zenodo.org/records/12805102> (2024).
60. Kawahara Y, Bastide M, Hamilton JP, Kanamori H, McCombie WR, Ouyang S, et al. Improvement of the *Oryza sativa* Nipponbare reference genome using next generation sequence and optical map data. *Rice*. 2013;6(1):4.
61. Zhao H, Li J, Yang L, Qin G, Xia C, Xu X, Su Y, Liu Y, Ming L, Chen L-L, Xiong L, Xie W. An inferred functional impact map of genetic variants in rice. *Mol Plant*. 2021;14(9):1584–99.
62. Andersen TB, Dalgaard CJ, Selaya P. Climate and the emergence of global income differences. *Rev Econ Stud*. 2016;83:rdw006.
63. Huang X, Zhao Y, Wei X, Li C, Wang A, Zhao Q, et al. Genome-wide association study of flowering time and grain yield traits in a worldwide collection of rice germplasm. *Nat Genet*. 2011;44(1):32–9.
64. Wang W, Mauleon R, Hu Z, Chebotarov D, Tai S, Wu Z, et al. Genomic variation in 3,010 diverse accessions of Asian cultivated rice. *Nature*. 2018;557(7703):43–9.

## Publisher's Note

Springer Nature remains neutral with regard to jurisdictional claims in published maps and institutional affiliations.